Document downloaded from:

http://hdl.handle.net/10251/47704

This paper must be cited as:

Gómez, C.; Culebras, M.; Cantero, A.; Redondo Foj, MB.; Ortiz Serna, MP.; Carsí Rosique, M.; Sanchis Sánchez, MJ. (2013). An experimental study of dynamic behaviour of graphite polycarbonatediol polyurethane composites for protective coatings. Applied Surface Science. 275:295-302. doi:10.1016/j.apsusc.2012.12.108.

The final publication is available at

http://dx.doi.org/10.1016/j.apsusc.2012.12.108

Copyright Elsevier

A Dielectric Study of Graphite-Polycarbonatediol Polyurethane Composites for Protective Coatings

C. M. Gómez[a,], M. Culebras[a], A. Cantarero[a], B. Redondo-Foj[b], P. Ortiz-Serna[b], M. Carsí[b], M. J. Sanchis[b]

[a]*Materials Science Institute, University of Valencia, P. O. Box 22085, 46071 Valencia, Spain*

[b]*Instituto de Tecnología Eléctrica, Departamento de Termodinámica Aplicada, ETSII, Universitat Politècnica de València, Valencia, Spain*

Abstract

Segmented polycarbonatediol polyurethane has been synthesized and modified with different amounts of graphite conductive filler (from 0 to 50 wt %). Thermal and Dynamical thermal analysis behavior of the composites clearly indicates the changes in polyurethane relaxations upon addition of graphite. Broadband Dielectric Spectroscopy has been used to study the dielectric properties of the composites in the frequency range from 10^{-2} to 10^{7} Hz and temperature window of -140 to 170 °C. Conductivity, relaxation processes associated with different molecular motions, Maxwell-Wagner-Sillars and electrode polarization are discussed and related with the graphite content.

Keywords: Dielectric, polyurethane, expanded graphite, composites

1. Introduction

In recent years, electrically conductive polymers have attracted a lot of attention because of their wide possible applications. Since polymers are, in general, insulating materials, many efforts have been directed to improve their electrical conductivity [1, 2, 3]. Electrically insulating polymers such as polyurethane can be specifically modified in order to increase its conductivity by dispersing conductive fillers [4, 5]. Polycarbonatediol polyurethanes are widely used as protective coatings for materials that are subjected to environmental degradation. The excellent properties of polyurethanes such as high impact resistance, high elasticity, resistance to corrosion, sunlight, oxidation

or weather conditions, made these polymers very useful as protective coatings [6, 7]. Another important property for coatings is the electrical conductivity. Conductive metals lack of properties such as elasticity and corrosion resistance. In contrast, insulating polymeric materials behave as conductive ones by addition of conductive particles, show good mechanical properties and are easy to mold. Carbon materials such as Carbon Nanotubes (CNTs) have been used to increase the electrical properties of polymer matrices [8]. However, CTNs are very expensive for large-scale applications. Other conductive fillers such as graphite and its variants are being used provide electrical conductive properties to polymeric matrices[9, 10]. Graphite, is very cheap, abundant, has an elevated electrical conductivity ($10^4\ S \cdot cm^{-1}$), and increases the mechanical properties of polymers having a reinforcing effect on the polymeric material [10]. The drawback is the difficult dispersion of the graphite in the polymer matrix fact that can be overcome by modifying its surface. For example, graphite can be expanded by chemical oxidation and thermal shock in order to increase the size of channels, improving thus the interaction with the polymer matrix [11]. In this work, polyurethane has been synthesized and modified with different amounts of expanded graphite (EG) as a conductive filler. The composites characterization has been carried out by means of thermogravimetric analysis, differential scanning calorimetry, wide angle X-ray diffraction, dynamic mechanical analysis and Broadband Dielectric Spectroscopy. The main goal of the present work is the study of these materials as potential candidates for coating applications.

2. Experimental

2.1. Materials

Polyhexamethylene-pentamethylene carbonatediol , PH100, was obtained from *UBE Chem Eur. (Castellon, Spain).* 4-4'-diphenylmethane diisocyanate, butanediol, natural graphite powder of size $< 20\ \mu$m, N,N Dimethylacetamide, nitric acid and sulfuric acid were purchased from Sigma-Aldrich Co (Madrid, Spain).

2.2. Preparation of expanded graphite

Expanded graphite was obtained by the method of chemical oxidation [11]. The natural graphite was dried at 75 °C in a vacuum oven for 10 h. Then, it was blended for 12 h with a 3:1 sulfuric and nitric mixture in order to form the graphite inserted compound. The nitric acid is used as an oxidizer

and the sulfuric acid as an intercalating agent. The mixture was stirred from time to time to get an uniform intercalation of the sulfuric into the graphite flakes. After that, the mixture was washed to obtain a neutral pH, then was filtered and the resulting material was dried at 60 °C in vacuum for 5 h. Afterwards it was subjected to a thermal shock at 800 °C for 20 s in order to form the expanded graphite.

2.3. Preparation of segmented polycarbonatediol polyurethane (PUPH)

Polyurethane solutions were obtained by a standard polymerization method based on the two-step process in dimethylacetamide [12]. In the first step one equivalent of policarbonatodiol PH100 were inserted in the reactor, previously dried for 24 hours at 100 °C, was inserted in the reactor with three equivalents of 4,4'-diphenylmethane diisocyanate. The reaction is carried out at 70 °C for 2 h under argon atmosphere. The second step corresponds to the addition of the chain extender, butanediol. Two equivalents of butanediol were added to obtain a viscous amber polyurethane solution with approximately 25 wt% in solid content. The solution is stored for 24 h in order to remove the bubbles produced in the synthesis process. Figure 1 shows a scheme of the chemical structure of PUPH.

2.4. Preparation of composites

Different weight fractions of expanded graphite, from 0 to 50 wt%, were introduced in the PUPH solution. In order to disaggregate the EG akes and to obtain a stable dispersion, the blend was sonicated in an ultrasonic bath for 1h and was stirred vigorously for 5 h, respectively. The suspensions were cast on glass slides which were previously washed in an ultrasonic bath with distilled water and later with acetone in order to eliminate the water. The polyurethane /expanded graphite composites (PUPH/EG) coated glasses were kept at 70 °C during 12 h. Films were prepared with dimensions of (4×2.7) cm^2 and with a thickness that ranged between 200-250 nm. An image of the PUPH and PUPH/EG solutions are shown in Figure 2.

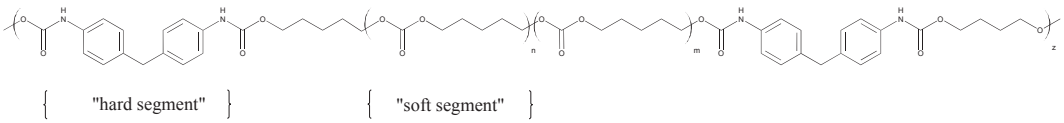

Figure 1: Scheme of the chemical structure of the segmented polyurethane in soft and hard segments.

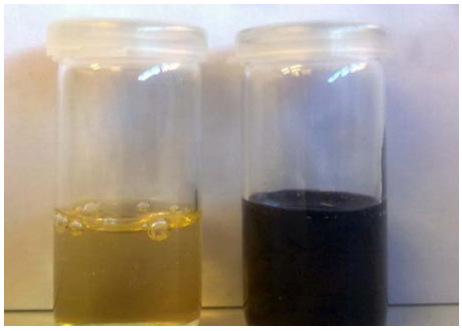

Figure 2: PUPH solution (left) and PUPH/EG solutions (right).

3. Characterization

3.1. Thermogravimetric Analysis

Thermogravimetric analysis (TGA) was performed on a Setaram Setsys 16/18 TGA-ATD analyzer. The samples were analyzed in platinum pans at a heating-cooling rate of 10 °C/min from 30 to 1000 °C under oxygen atmosphere. Samples masses ranged from 7 to 10 mg.

3.2. Differential Scanning Calorimetry measurements

Differential scanning calorimetry (DSC) study was performed on a Q-20 differential scanning calorimeter from TA Instruments calibrated with indium. The measurements were carried out in the range of -90 to 220 °C at a heating rate of 20 °C/min under nitrogen atmosphere. A second run (to delete the thermal history) was used for the thermal characterization of the films.

3.3. X-ray characterization

The wide angle X-ray diffraction (WAXRD) was acquired on a Bruker AXS D5005 diffractometer. The samples were scanned at 4 °C/min using Cu K_α radiation ($\lambda = 0.15418$ nm) at a filament voltage of 40 kV and a current of 20 mA. The diffraction scans were collected within the range of $2\theta = 5 - 80°$ with a 2θ step of 0.01°.

3.4. Dynamic mechanical measurements

Dynamic mechanical measurements (DMA) were performed on a 2980 dynamic mechanical analyzer (TA instruments). The temperature range went from -100 to 180 °C by using rectangular samples of dimension (16.540 x 6.000 x 0.250) mm^3. Measurements were carried out at 3 °C/min heating rate and at a frequency of 1 Hz.

3.5. Dielectric measurements

The experimental dielectric behavior (DRS) of PUPH and PUPH/15EG films was studied with a Novocontrol Broadband Dielectric Spectrometer (Hundsagen, Germany) consisting of an Alpha analyzer to carry out measurements from $5 \cdot 10^{-2}$ to $3 \cdot 10^6$ Hz. The measurements were carried out in inert N_2 atmosphere between -150 to 150 °C. The temperature was controlled by a nitrogen jet (QUATRO from Novocontrol) with a temperature error of 0.1 °C during each single sweep in frequency. Molded disc shaped samples of about 0.1 μm thickness and 20 mm diameter were used. The experimental uncertainty was better than 5 % in all cases.

4. Results and discussion

Thermogravimetric analysis was carried out in order to analyze the effect of expanded graphite insertion on the stability of the polyurethane films. This analysis allows the evaluation of changes in weight as a function of temperature in a controlled atmosphere. Figure 3 shows the TGA thermograms obtained for each film and Table 1 collects the characteristic temperatures of the degradation processes in the materials under study. T_{on} is the temperature related to beginning the decomposition process, T_p is the temperature the maximum rate of weight loss and T_{end} is the temperature related to the ending of decomposition process ending. For PUPH films two degradation processes have been observed. The first starts around 312 °C and it is due to urethane bound decomposition. The second process that appears near 486 °C, is related with a weight loss associated with other segments of the remaining structure or with a probable C-C bound cleavage [13, 14]. In the case of EG particles only one degradation process has been observed. This process begins at 609 °C ais related to the carbon atoms oxidation in the EG particles. In PUPH/EG films three degradation processes can be observed. The two first are related with the degradation of the polymer matrix and the last process is due to the degradation of the EG particles. According to our results, the EG particles have not a signicant effect on the PUPH/EG composites stability, because the characteristic temperatures of degradation processes are very similar in the films with and without EG. Instead the presence of polymer chains decreases the degradation temperature of EG particles as shown in Table 1. A similar effect has been observed in other composites [15].

Table 1: Thermogravimetric characteristic temperatures of PUPH/EG composites.

% EG	T_{on1} (°C)	T_{p1} (°C)	T_{end1} (°C)	T_{on2} (°C)	T_{p2} (°C)	T_{end2} (°C)	T_{on3} (°C)	T_{p3} (°C)	T_{end3} (°C))
0	312	349	370	486	501	537			
15	308	341	361	460	503	538	578	610	676
30	311	345	363	470	507	531	562	588	680
50	310	352	368	486	510	532	555	580	693
100							609	649	755

In order to study the thermal behavior of the PUPH and PUPH/EG composites, DSC measurements were carried out in the temperature range

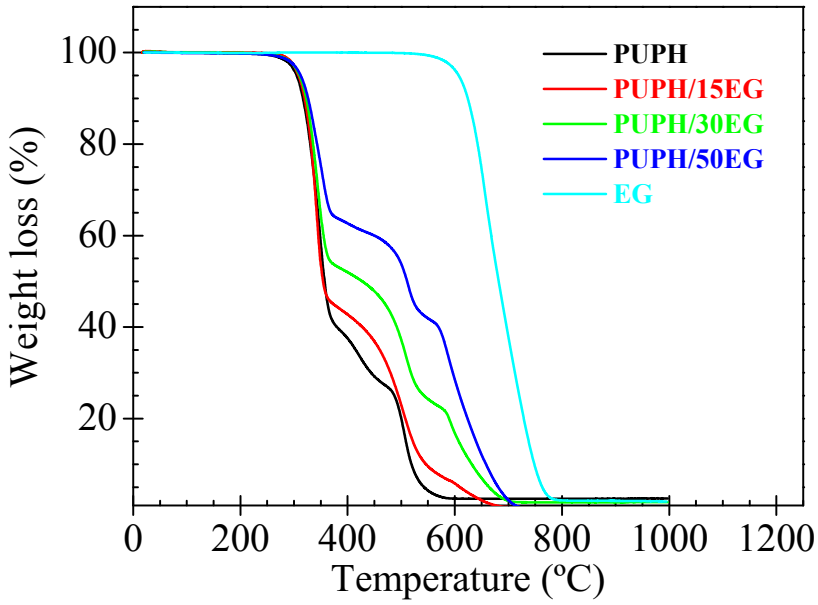

Figure 3: Weight loss as a function of temperature for PUPH/EG composites.

from -90 to 220 °C. The DSC thermograms obtained for PUPH/EG samples are shown in Figure 4 and the characteristic parameters obtained are summarized in Table 2. These parameters are: the initial and nal temperature of the transition, T_1, and T_2, the glass transition temperature, T_g, the variation of the heat capacity, ΔC_{pnor}, the melting temperature, T_c, and the degree of crystallinity, χ_c, determined from the enthalpy of crystallization normalized using $\chi_c = \Delta H_c / \Delta H_{100\%}$, where ΔH_c is the enthalpy of fusion of every sample and $\Delta H_{100\%}$ is the enthalpy of fusion of the hard segment, taken as 25.85 J/g. For all the analyzed samples, the glass transition temperature (T_g), evaluated as the midpoint of the specic heat capacity increment, appears in the temperature range from -20 to 10 °C, and the melting peak is visible around 187 °C.

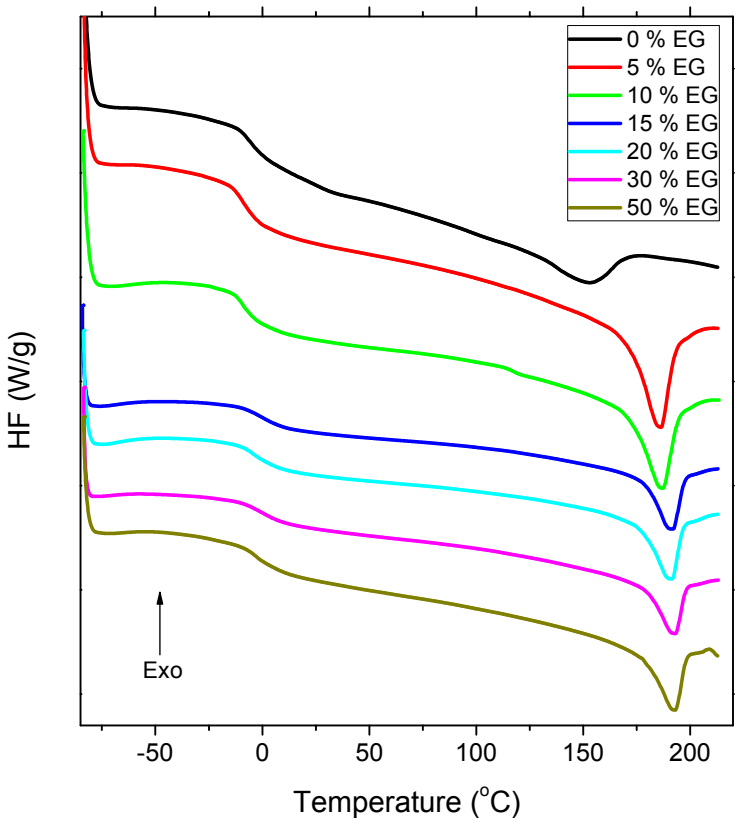

Figure 4: DSC curves taken at 20°C/min of the PUPH/EG composites.

Depending on the EG content two different trends are observed in the values of the glass transition temperatures. Thus, for low EG particles content, a decrease of T_g is observed, which indicates that the EG addition tends to increase mobility. The PUPH with a 5 wt% of EG has a T_g of -8.9 °C, which is even lower than the PUPH T_g (-4.8 °C). It seems that the presence of EG moiety in the composites is unable to increase the T_g of the parent polymer. This tendency is probably associated with an increase of the free volume due to loosened molecular packing of the chain. So, the presence of EG particles, at a relative smaller content, reduces the dipole-dipole interactions of PUPH

molecules and, plays an inert diluent role to decrease the self-association interaction of PUPH molecules. Similar tendency has been observed in other composites[16, 17, 18, 19, 20].However, for high content (15-30 wt%) of EG particles, an increase in the T_g is observed. This can be associated with the reduction of molecular mobility of the polyurethane chains imposed by the EG particles. That is a fraction of polymer could be immobilized on the surface of the EG particles [21, 22, 23, 24, 25, 26, 27].

Table 2: Parameters obtained from DSC of PUPH/EG composites.

% EG	T_1 (°C)	T_2 (°C)	($T_2 - T_1$) (°C)	T_g (°C)	ΔC_{pnor} J/g °C	T_c (°C)	χ_c (%)
0	-10.4	0.4	10.8	-4.8	0.1784	153.0	14.9
5	-13.7	-3.7	10.7	-8.9	0.208	186.0	37.7
10	-12.3	-3.9	8.4	-9.6	0.165	187.0	36.8
15	-7.3	8.7	16.0	-1.0	0.191	191.0	38.5
20	-9.3	1.1	10.4	-4.0	0.142	191.3	37.1
30	-6.6	8.3	14.9	-0.4	0.147	192.8	35.0
50	-6.6	3.0	9.6	-3.1	0.061	192.6	30.4

The temperature range of the glass transition ($T_2 - T_1$), which is a measure of the sample heterogeneity [18], does not show a clear trend with the composition. So, according to our results, for the composites with low EG content (5-10 wt%), the temperature range of the glass transition decreases with the EG content. However, for the composites with 15 wt% and 30 wt% EG content, this temperature range signicantly increases significantly. On the other hand, the heat capacity jump at T_g, normalized to the fraction of PUPH, which is a measure of the fraction polymer participating in the glass transition, systematically decreases with the EG content. Similar results have been obtained also for other polymer composites [28], and can be interpreted in terms of the amount of the amorphous polymer which makes non contribution to the glass transition. Therefore it is related to the fraction of polymer being immobilized on the surface of the EG particles [18, 29]. This fraction increases with the EG content, excepting for the sample with 15 wt% wt of EG, in which case the obtained value shows the opposite effect. The analysis shows that the melting temperature, T_c increases with the EG content. The degree of crystallinity, shown in Table 2 is 14.9% for the pure PUPH, and increases with the filler content up to 15 wt%, suffering a

reduction for higher contents of EG. This is an indication that from a certain concentration of EG particles, the creation of crystallization nuclei is restricted.

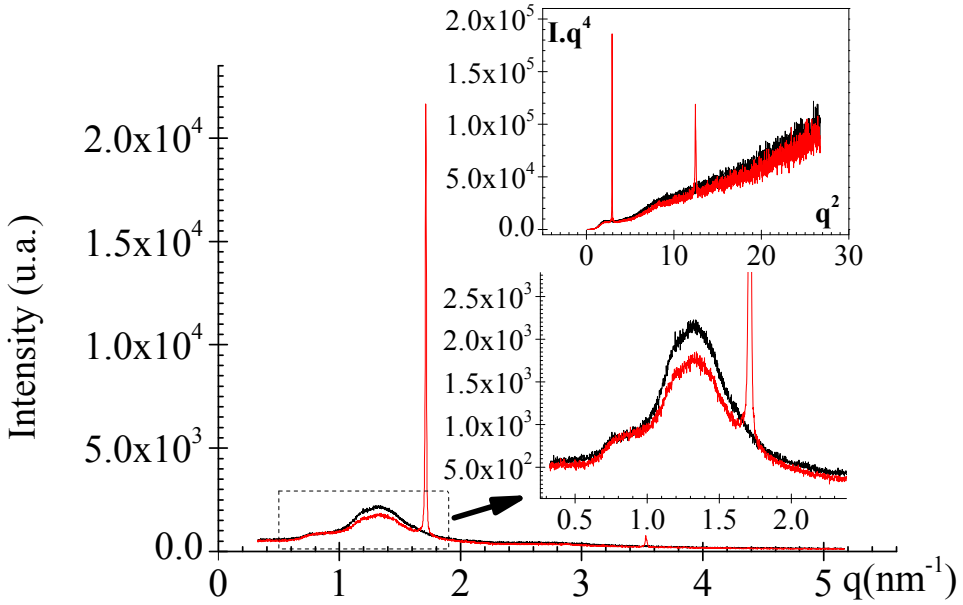

Figure 5: X-ray diffraction pattern for PUPH (black curve) and PUPH/15EG (red curve).

The X-ray patterns obtained for PUPH and PUPH/15EG composite are shown in Figure 5. The spectra show the presence of a broad peak centered in the vicinity of $q = 1.31$ nm^{-1} ($2\theta = 20.65°$) and a small shoulder at q=0.8 nm^{-1} ($2\theta = 12.6°$). These peaks are ascribed to the micro-phase separated morphology into "soft" and "hard" phases occurring during polymerization and are an indication of short range order commonly sees in polyurethanes [30, 31]. Also, for PUPH/15EG at q=1.87 nm^{-1} ($2\theta = 26.5°$) a narrow diffraction peak associated with the expanded graphite it is observed. The plot of $I \cdot q^4$ vs q^2 for PUPH and PUPH/15EG exhibits a positive slope (see inset in Figure 5). This behavior is called as a positive deviation from Porod's law [32], and is typical of multi-phase polymeric systems containing thermal density fluctuations and diffuse phase boundaries. The inter-domain spacing, d, which only depends on the molecular weight of the macrodiol, was estimated using Bragg's law to be equal at a value of d ca. 5 nm. Accordingly,

interfaces in the nano-domains of PUPH and PUPH/15EG may condition charge transport in the polymer melts at low frequencies, as discussed below. It should be noted that the intensity of the peak at $2\theta = 20.65^{\circ}$ decreases significantly after EG incorporation but the small shoulder remains constant. This intensity reduction reflects, in some way, an eventual reduction in the number of existing nano-domains in the film. So, according to the WAXRD results, incorporation of EG governs the polymer chain movement and consequently molecule polarization, which is important to the dielectric properties, and will be discussed later.

DMA analysis were performed in order to determine the viscoelastic properties of PUPH and PUPH/EG films. Figure 6 shows the storage modulus, E', and loss modulus, E'' as a function of temperature. The storage modulus increases as the EG content increases suggesting that the particles of expanded graphite have a reinforcing effect on the polyurethane matrix. The temperature of the maximum of E'' is related to the T_g of the material and shifts to higher values as the EG content increases. Similar trend is observed in the DSC experiments.

Figure 7 shows the temperature dependence of the dielectric permittivity and loss factor at several frequencies for the PUPH and PUPH/15EG films. In order to a clear visualization of the samples behavior with temperature, Figure 8a plots the real and imaginary part of the complex permittivity as a function of the temperature at 1 Hz. The isochrone that shows the temperature dependence of ε' presents two steps. At low temperatures a rst step associated with the glass rubber or α relaxation is followed by a second step at higher temperatures, associated with the Maxwell-Wagner-Sillars (MWS) relaxation. Finally, at the higher temperatures an important increase of the permittivity related with the electrode polarization (EP) effects is observed. The second step is more clearly visualized for the PUPH film, since for the PUPH/EG composites the EP process is more important and makes difficult the MWS process denition. EP process proceeds from the accumulation of charges at the electrodes-polymer interface, whereas the interfacial polarization or MWS process is due to the build-up of charges at the interfaces of components of heterogeneous systems. The PUPH is a heterogeneous system due to the existence of micro-phase separation associated with the *"soft"* and *"hard"* micro-domains. The polarization of micro-domains resulting from the separation of the *"hard"* and *"soft"* segments of PUPH chains can cause the accumulation of charges, a process that can be attributed to the different conductivity between *"soft"* and *"hard"* micro-domains. Probably

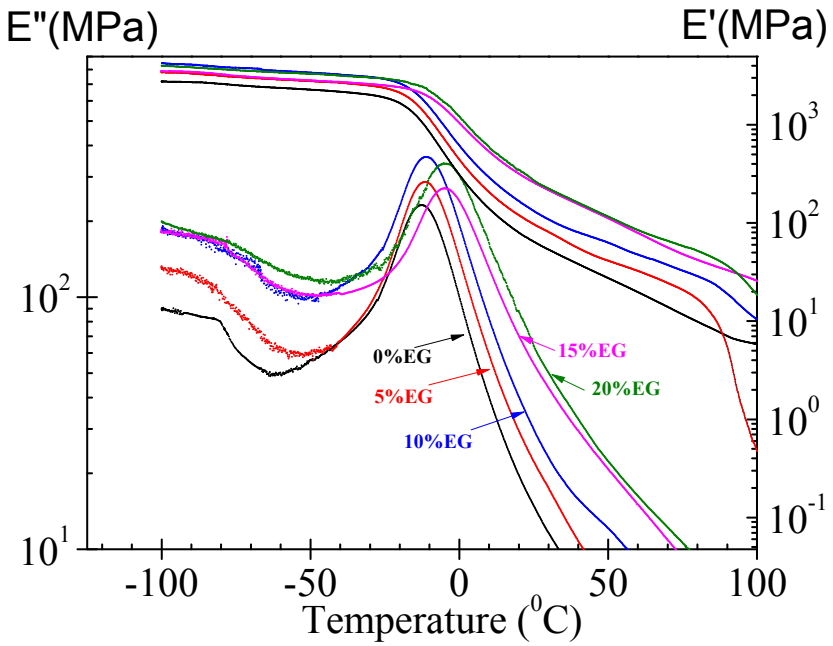

Figure 6: Temperature dependence of storage and loss modulus for the PUPH/EG composites at 1 Hz.

these micro-domains are the responsible of the observed MWS process. The α relaxation appears at high temperatures with the increasing of EG content, indicating a mobility in the polymer chains. This result is in agreement with the DSC and DMA results previously reported, which show an increase in the T_g upon addition of 15% wt of EG particles. Low temperature spectrum shows the presence of almost two secondary processes. These processes seem to be unaffected the by addition of EG, as can be expected due to their local character.

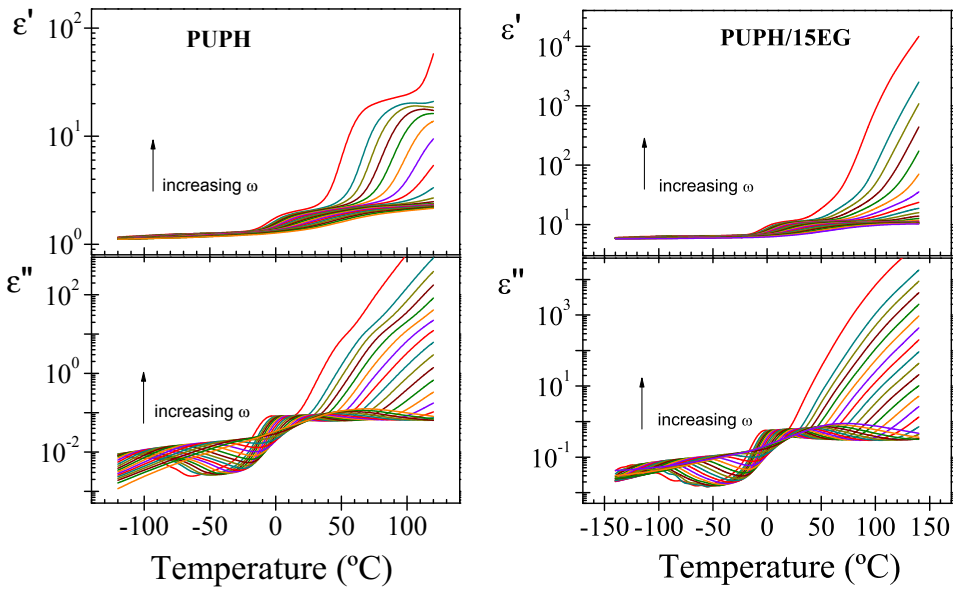

Figure 7: Temperature dependence of the permittivity (ε') and loss factor (ε'') for PUPH100 and PUPH/15EG at several frequencies.

To get insight of the complex conductive behavior of the films, it is advisable to use the electric modulus formalism ($M^{=}1/\varepsilon$) for the data representation. This formalism has several advantages, namely,(i) it allows the determination of the dc conductivity from the M'' spectra, since the EP effects often do not mask the features of the spectra, and (ii) the results of the analysis are seemingly analogous tothose of the mechanical modulus of solids. As we can see in Figure 8b, better definitions of the loss peaks are obtained by plotting the dielectric results in terms of the dielectric loss modulus, M''. The isochrone of M'' exhibits three ostensible peaks corresponding in increasing order of temperature to the overlapped secondary relaxations (β and γ), the α-relaxation and the MWS process overlapped with the EP process in the high temperature region. The last process is better visualized, as a peak, in the tan δ representation as we can observe in Figure 8c.

For a clear visualization, the dielectric permittivity and loss factor of PUPH and PUPH/15EG were also plotted in the frequency domain in Figure

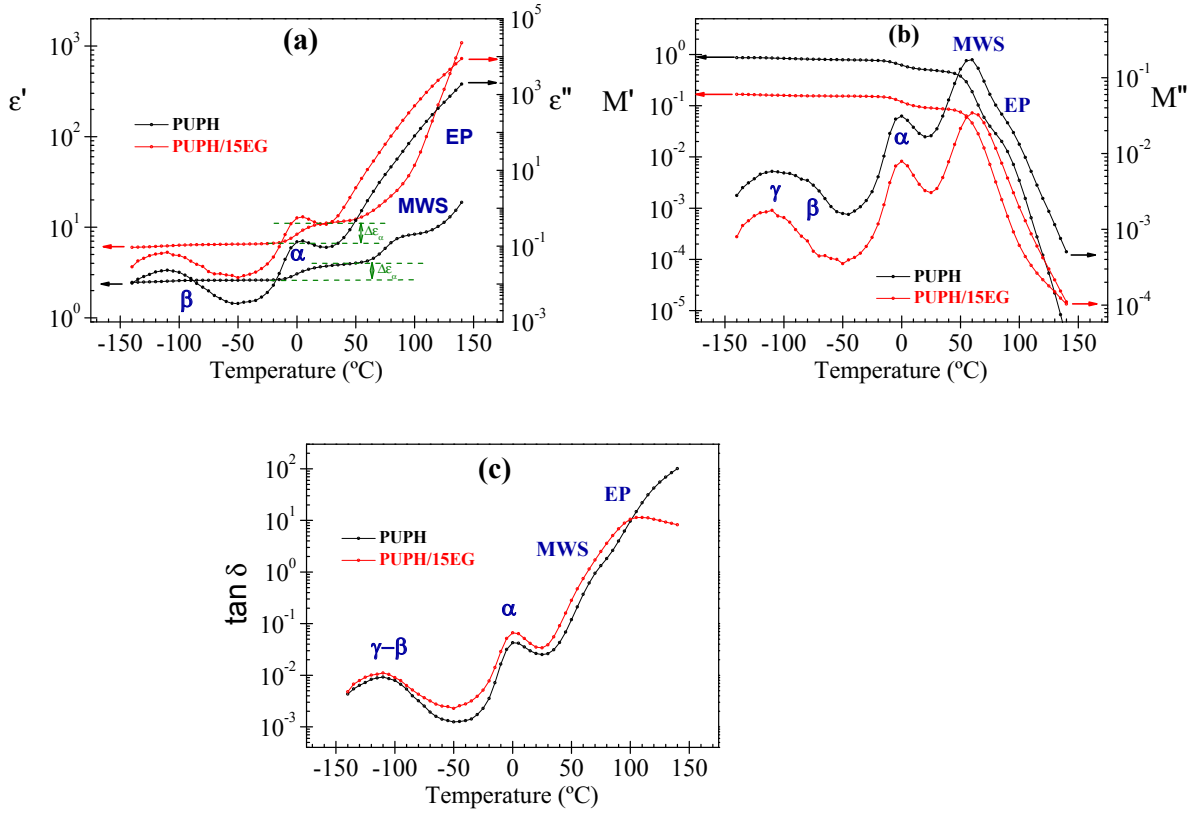

Figure 8: Temperature dependence of (a) the permittivity (ε')/loss factor (ε''), (b) modulus (M') and loss modulus (M") and (c) tan δ for PUPH (black curve) and PUPH/15EG (red curve) at 1 Hz.

9. As we can see, the MWS process related to the nanodomains formation of *"soft"* and *"hard"* segments is hindered by the inclusion of EG filler. Figure 10 shows the frequency dependence of the dielectric loss modulus at 0 and 80 °C. The α relaxation becomes slower with increasing EG content, indicating a reduced mobility in the composites. This result is in agreement with the DSC and DMA results previously reported, which show an increase of the T_g upon addition of EG particles. On the other hand, the relaxation strength increases significantly in the composite ($\Delta\varepsilon_{PUPH} \sim 1.3$ front $\Delta\varepsilon_{PUPH/15EG} \sim 4.9$). This increase may be due to the reduction of the immobilized polymer fraction. Significant effect of EG content is observed on the definition of the MWS process pointing out of showing that the micro-phase-separated

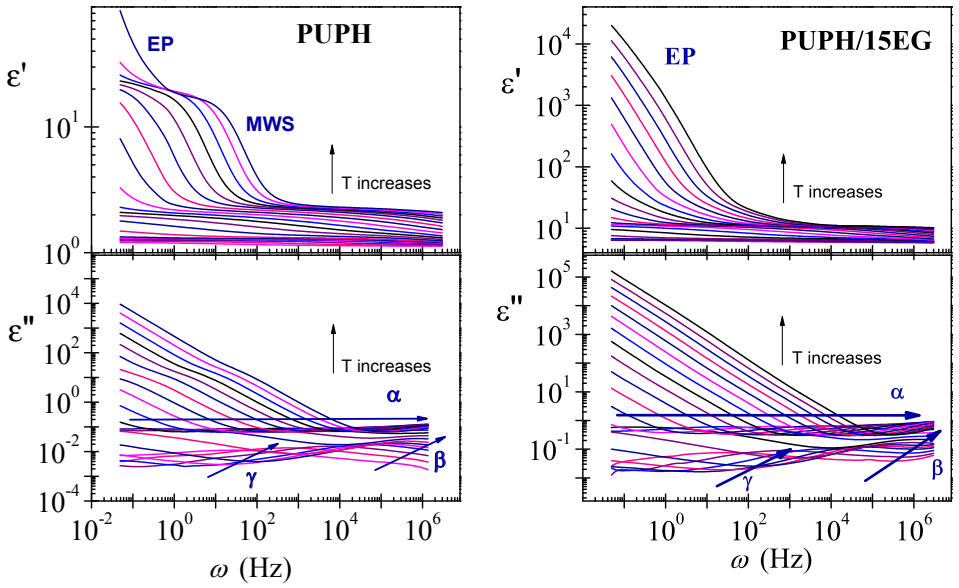

Figure 9: Dielectric Permittivity (ε') and loss factor (ε'') as a function of frequency for PUPH and PUPH/15EG films in the temperature range -100-120 °C.

morphology of the PUPH matrix is significantly modified with the addition of EG.

The ac conductivity has been calculated from the dielectric permittivity according to the relationship:

$$\sigma^* = j\omega e_0 \varepsilon^*(\omega) \tag{1}$$

In general at a constant temperature, the ac conductivity can be expressed as[33, 34]

$$\sigma(\omega) = \sigma_{dc} + A\omega^s \tag{2}$$

where σ_{dc} is the $\omega \to \infty$ limiting value of $\sigma(\omega)$ and A, s are parameters depending on the temperature. Equation (2) is often called "the ac universality law" since it has been found to satisfactorily describe the ac response of numerous different types of materials, which can be classified as disordered solids [34, 35, 36].

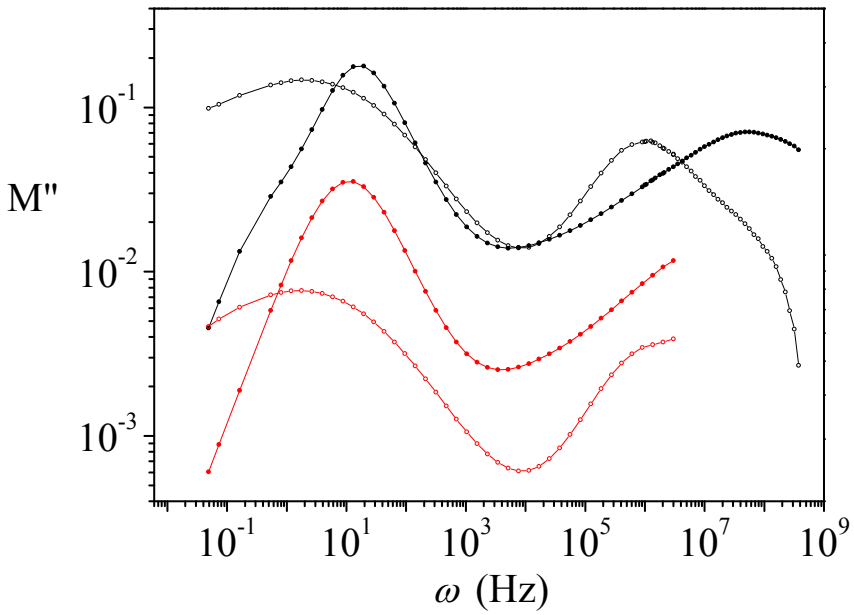

Figure 10: Frequency dependence of the dielectric loss modulus at 0 (open symbols) and 80 °C (full symbols) for PUPH (black curve) and PUPH15EG (red curve).

Figure 11 depicts the frequency dependence of the ac conductivity at several temperatures in the range from 45 to 140 °C (5 °C step).

In the low frequency and high temperature zone, a frequency independent conductivity is recorded, which is attributed to resistive conduction through the bulk of polymer. On the other hand, when frequency is raised, the main displacement of the charge carriers is reduced, and the conductivity appears to be proportional to the frequency following the law $\sigma'_{ac}(\omega) \propto \omega^s$ with $0 \leqslant s \leqslant 1$ characterizing hopping conduction. As expected, the EG particles inclusion produces an increase in the electrical conductivity of the films. The inset of Figure 11 shows the values of dc conductivity, obtained from extrapolations at low frequencies, as a function of the temperature reciprocal. As we can see, the dc conductivity is thermally activated and can be described by

$$\sigma_{dc} = \sigma_0 \cdot e^{\frac{-E_a}{RT}} \tag{3}$$

The corresponding activation energies are $108 \pm 1(PUPH)$ and $95.2 \pm$

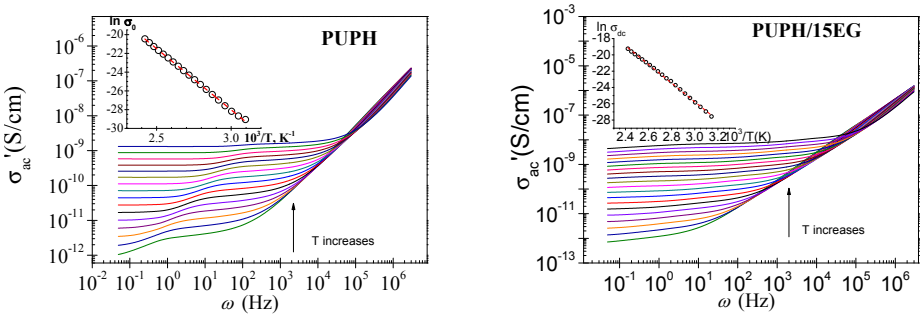

Figure 11: *ac* conductivity against frequency for PUPH and PUPH/15EG at temperatures in the range of 45°C to 140°C (step 5°C). Inset: Arrhenius plot of *dc* conductivity.

$0.8kJ/mol(PUPH/15EG)$, pointing out the similar origin of the conductivity process in both films.

Table 3: Parameters of equation and σ_{dc} at 25 °C

EG %	E_a $(kJ \cdot mol^{-1})$	ln σ_0 $(S \cdot cm^{-1})$	$\sigma_{dc}^{25°C}$ $(S \cdot cm^{-1})$
0	108 ± 1	10.9 ± 0.3	$7.564 \cdot 10^{-15}$
15	95.2 ± 0.8	8.6 ± 0.3	$1.110 \cdot 10^{-13}$

5. Conclusions

The obtained results obtained from the thermogravimetric analysis indicate that inclusion of EG particles does not significantly increases the thermal stability of the polyurethane matrix. However, expanded graphite reduces its temperature decomposition in presence of polyurethane. The mechanical and dielectric results provide a reasonable explanation of the improved thermal stability of the composites in terms of the segmental dynamics restriction. The physical properties of polyurethanes (PUPHs), like glass transition temperature (T_g), strongly depend on the degree of the micro-phase separation. In our case, only one T_g was observed in the analyzed films. For low EG content a decrease of the T_g value of the composite is observed. This behavior is associated with an increase of the free volume due to loosened molecular packing of the chain, resulting in an increase of the molecular mobility. Besides, for high EG contents, the interaction between PUPH-EG produces a reduction of the molecular mobility and therefore an increase in T_g. The

higher value of the ΔC_{pnor} for the PUPH/15EG composite, associated with an increase of the fraction of polymer contributing to the glass transition, is in accordance with the dielectric/mechanical results. So, the strength of segmental relaxation was increased upon addition of 15 wt% of EG, indicating an increase of the polymer fraction participating in the glass transition temperature. This can be interpreted as the reorganization imposed for the EG particles, that leads to the loosening of the crystalline constraint imposed on the amorphous phase. Two kinds of interfaces coexist in PUPH/EG composites, those between soft and hard segments in amorphous regions and those between polymer and EG particles. The MWS process is more important for PUPH than for PUPH/15EG, which might indicates a qualitative change of the morphology with the composition. The crystalline phase and EG particles, probably preclude the formation of nano-domains of *"soft"* and *"hard"* segments responsible of the MWS process. The presence of EG particles produces an enhancement of trapping of charge carriers. Thus, increasing the electrical conductivity.

We acknowledge the financial support of the Ministry of Finances and Competitiveness through the Grant CDS2010-0044 belonging to the "Consolider-Ingenio Programme" and for the Grant MAT2012-33483. The authors thank UBE Chem Eur for the PCD supply for this work.B.R.F, M.C, P.O. and M.J.S., gratefully acknowledge to CICYT for grant MAT2008-06725-C03.

6. References

[1] J.-C. Zhao, F.-P. Du, X.-P. Zhou, W. Cui, X.-M. Wang, H. Zhu, X.-L. Xie, Y.-W. Mai, Thermal conductive and electrical properties of polyurethane/hyperbranched poly(urea-urethane)-grafted multi-walled carbon nanotube composites, Compos. Pt. B-Eng. 42 (2011) 2111–2116.

[2] G. Chen, C. Wu, W. Weng, D. Wu, W. Yan, Preparation of polystyrene/graphite nanosheet composite, Polymer 44 (6) (2003) 1781–1784.

[3] F. El-Tantawy, K. Kamada, H. Ohnabe, A novel way of enhancing the electrical and thermal stability of conductive epoxy resin-carbon black composites via the joule heating effect for heating-element applications, J. Appl. Polym. Sci. 87 (2003) 97–109.

[4] G. Otieno, J.-Y. Kim, Conductive graphite/polyurethane composite films using amphiphilic reactive dispersant: Synthesis and characterization, J. Ind. Eng. Chem. 14 (2) (2008) 187–193.

[5] H. Chang, Y.-M. Yeh, K.-D. Huang, Electromagnetic Shielding by Composite Films Prepared with Carbon Fiber, Ni Nanoparticles, and Multi-Walled Carbon Nanotubes in Polyurethane, Mater. Trans. 51 (2010) 1145–1149.

[6] Y. Zhu, J. Xiong, Y. Tang, Y. Zuo, EIS study on failure process of two polyurethane composite coatings, Prog. Org. Coat. 69 (2010) 7–11.

[7] V. Garcia-Pacios, V. Costa, M. Colera, J. Miguel Martin-Martinez, Waterborne polyurethane dispersions obtained with polycarbonate of hexanediol intended for use as coatings, Prog. Org. Coat. 71 (2011) 136–146.

[8] I. Sandu, M. Brasoveanu, I. Morjan, I. Voicu, F. Dumitrache, C.-F. Teodor, L. Gavrila-Florescu, Synthesis of optical transparent and electrical conductive polymer/nanocarbon composite films by infiltration method, Thin Solid Films. 519 (12, SI) (2011) 4128–4131.

[9] S. Konwer, J. Maiti, S. K. Dolui, Preparation and optical/electrical/electrochemical properties of expanded graphite-filled polypyrrole nanocomposite, Mater. Chem. Phys. 128 (2011) 283–290.

[10] F. He, J. Fan, S. Lau, Thermal, mechanical, and dielectric properties of graphite reinforced poly(vinylidene fluoride) composites, Polym. Test. 27 (2008) 964–970.

[11] S. R. Dhakate, S. Sharma, M. Borah, R. B. Mathur, T. L. Dhami, Expanded graphite-based electrically conductive composites as bipolar plate for PEM fuel cell, Int. J. Hydrog. Energy 33 (2008) 7146–7152.

[12] B. F. D'Arlas, L. Rueda, K. De la Caba, I. Mondragon, A. Eceiza, Microdomain composition and properties differences of biodegradable-polyurethanes based on MDI and HDI, Polym. Eng. Sci. 48 (3) (2008) 519–529.

[13] K. Pielichowski, J. Pielichowski, A. Prociak, Chlorinated polyurethanes based on 2,4-toluenediisocyanate: Thermalanalysis and flammability evaluation, J. Appl. Polym. Sci. 67 (8) (1998) 1465–1471.

[14] Z. Petrovic, Z. Zavargo, J. Flynn, W. Macknight, Thermal-degradation of segmented polyurethanes, J. Appl. Polym. Sci. 51 (6) (1994) 1087–1095.

[15] D. H. Wang, S. Sihn, A. K. Roy, J.-B. Baek, L.-S. Tan, Nanocomposites based on vapor-grown carbon nanofibers and an epoxy: Functionalization, preparation and characterization, Eur. Polym. J. 46 (7) (2010) 1404–1416.

[16] H. Xu, S. Kuo, J. Lee, F. Chang, Preparations, thermal properties, and T-g increase mechanism of inorganic/organic hybrid polymers based on polyhedral oligomeric silsesquioxanes, Macromolecules 35 (2002) 8788–8793.

[17] B. Ash, L. Schadler, R. Siegel, Glass transition behavior of alumina/polymethylmethacrylate nanocomposites, Mater. Lett. 55 (2002) 83–87.

[18] V. Bershtein, L. Egorova, P. Yakushev, P. Pissis, P. Sysel, L. Brozova, Molecular dynamics in nanostructured polyimide-silica hybrid materials and their thermal stability, J. Polym. Sci. Pt. B-Polym. Phys. 40 (2002) 1056–1069.

[19] V. Arrighi, I. McEwen, H. Qian, M. Prieto, The glass transition and interfacial layer in styrene-butadiene rubber containing silica nanofiller, Polymer 44 (2003) 6259–6266.

[20] B. Ash, R. Siegel, L. Schadler, Glass-transition temperature behavior of alumina/PMMA nanocomposites, J. Polym. Sci. Pt. B-Polym. Phys. 42 (2004) 4371–4383.

[21] K. Chen, S. Yang, Synthesis of epoxy-montmorillonite nanocomposite, J. Appl. Polym. Sci. 86 (2002) 414–421.

[22] X. Liu, Q. Wu, PP/clay nanocomposites prepared by grafting-melt intercalation, Polymer 42 (2001) 10013–10019.

[23] A. Sargsyan, A. Tonoyan, S. Davtyan, C. Schick, The amount of immobilized polymer in PMMA SiO(2) nanocomposites determined from calorimetric data, Eur. Polym. J. 43 (2007) 3113–3127.

[24] V. P. Privalko, G. V. Titov, The heat capacity of filled, amorphous polymers, Pol. Sci. USSR 21 (1979) 380–387.

[25] X. Huang, W. Brittain, Synthesis and characterization of PMMA nanocomposites by suspension and emulsion polymerization, Macromolecules 34 (2001) 3255–3260.

[26] Y. S. Lipatov, V. P. Privalko, Glass transition in filled polymer systems, Pol. Sci. USSR 14 (1972) 1843–1848.

[27] I. Kalogeras, E. Neagu, Interplay of surface and confinement effects on the molecular relaxation dynamics of nanoconfined poly(methyl methacrylate) chains, Eur. Phys. J. E 14 (2004) 193–204.

[28] D. Fragiadakis, P. Pissis, Glass transition and segmental dynamics in poly(dimethylsiloxane)/silica nanocomposites studied by various techniques, J. Non-Cryst. Solids 353 (2007) 4344–4352.

[29] P. Klonos, A. Panagopoulou, L. Bokobza, A. Kyritsis, V. Peoglos, P. Pissis, Comparative studies on effects of silica and titania nanoparticles on crystallization and complex segmental dynamics in poly(dimethylsiloxane), Polymer 51 (2010) 5490–5499.

[30] F. S. Bates, G. H. Fredrickson, Block copolymer thermodynamics - Theory and experiment, Annu. Rev. Phys. Chem. 41 (1990) 525–557.

[31] A. J. Ryan, C. W. Macosko, W. Bras, Order-disorder transition in a block copolyurethane, Macromolecules 25 (1992) 6277–6283.

[32] G. Porod, Die Rotgenkelinwinkelstreuung von dichgepackten kolloiden systemen .1., Kolloid Zeit. & Zeit. Polymere 124 (1951) 83–114.

[33] H. Böttger, V. V. Bryksin, Hopping conduction in solids, Physical research, Akademie-Verlag, 1985.

[34] A. K. Jonscher, Universal relaxation law: a sequel to dielectric relaxation in solids, Chelsea Dielectrics Press, 1996, Ch. 5.

[35] J. C. Dyre, T. B. Schrøder, Universality of ac conduction in disordered solids, Rev. Mod. Phys. 72 (2000) 873–892.

[36] J. C. Dyre, The random free-energy barrier model for ac conduction in disordered solids, J. Appl. Phys. 64 (1988) 2456–2468.